Available online at www.sciencedirect.com

ScienceDirect

Energy Procedia 129 (2017) 184–191

Energy Procedia

www.elsevier.com/locate/procedia

IV International Seminar on ORC Power Systems, ORC2017
13-15 September 2017, Milano, Italy

Model Predictive Control of an Organic Rankine Cycle System

Xiaobing Liu[a,]*,Adamu Yebi[b], Paul Anschel[a], John Shutty[a], Bin Xu[b], Mark Hoffman[b], Simona Onori[b]

[a]BorgWarner Inc.,3800 Automation Ave., Auburn Hills, MI 48326, USA
[b]Clemson University, 4 Research Dr, Greenville, SC 29607, USA

Abstract

Organic Rankine Cycle (ORC) waste heat recovery systems offer promising engine fuel economy improvements for heavy-duty on-highway trucks. An ORC test rig with parallel evaporators to recover both tailpipe and EGR waste heat from a 13L heavy duty diesel engine was developed and used in this work to demonstrate a novel control strategy based on Model-Predictive Control (MPC). The main control objectives for the ORC system are: (i) regulation of working fluid temperature, (ii) safe turbine operation - away from 2-phase region, and (iii) maximization of waste heat recovery. The MPC uses a built-in moving boundary evaporator model to predict future system response and generate optimal actuator reference commands. Two variants of MPC were considered in this work: an adaptive linear MPC (LMPC) and a nonlinear MPC (NPMC). Compared with the traditionally used PID controller, MPC demonstrates more accurate temperature control and improved disturbance rejection in simulation. Finally, the LMPC and NMPC controllers were implemented on the ORC test rig and showing promising initial test results.

Keywords: Model Predictive Control; Waste Heat Recovery; Organic Rankine Cycle

1. Introduction

With tightening emission regulation on heavy-duty on-road vehicles, engine waste heat recovery technologies have been under extensive study in recent years. Organic Rankine Cycle (ORC) is a promising waste heat recovery technology providing about 3-5% fuel economy benefit in addition to base engine efficiency improvement [1]. In the SuperTruck program, Cummins reported a 3.6% absolute improvement in brake thermal efficiency of a heavy duty truck engine due to ORC with EGR and exhaust tailpipe evaporators [2]. ORC is similar to the conventional

* Corresponding author. Tel.: +1-248 754 0514
E-mail address: xliu@borgwarner.com

1876-6102
10.1016/j.egypro.2017.09.109

steam cycle used in power plants, except an organic fluid, such as ethanol, replaces water as working fluid due to the low-temperature heat source. The main challenge of operating an ORC in automotive applications is handling the highly transient and wide ranging engine operating conditions. This poses challenges on the ORC control system design. Tona and Peralez [3] presented a literature review on different ORC system architectures and control strategies used for heavy-duty vehicles. The ORC control approaches can be classified into two categories:

- traditional PID-based, e.g., PI feedback plus feedforward [4], PI-based decentralized control [5]
- advanced Model Predictive Control (MPC) [6,7,8]

Advanced MPC demonstrates better performance in simulation, but real-time implementation and validation on test rigs are scarce in literature if not absent at all. In this paper, the implementation of an adaptive linear MPC (LMPC) and a nonlinear MPC (NMPC) are described. Both simulation and preliminary experimental results are presented.

The paper is organized as follows. Section 2 describes the layout and main components of the ORC system. Section 3 presents the ORC control goals and challenges. Section 4 describes a PID controller implementation. Section 5 presents the MPC control structure, formulation, and evaporator modeling. Section 6 provides a comparison of MPC vs PID simulation results, and initial MPC test results. Finally, conclusions and future work are presented in Section 7.

2. System Description

2.1. ORC system layout

In order to provide OEMs with ORC components optimized for the engine application environment, BorgWarner has taken a “Systems Approach” to refine the ORC components via on-engine transient testing. An ORC test rig with parallel evaporators to recover both tailpipe (TP) and Exhaust Gas Recirculation (EGR) waste heat was developed to evaluate the dynamic requirements of ORC systems and refine the products accordingly. Fig. 1a shows a simplified schematic of the ORC system [6]. Major components in the system include: 2-stage pumps, two flow distribution valves, two evaporators in parallel, a turbine expander, a motor/generator, a condenser, and an exhaust gas bypass valve. The pumps increase the working fluid pressure up to 40bar and circulates working fluid through the evaporators. The low pressure feed pump is upsteam of the positive displacement type high pressure pump to prevent cavitation. The distribution valves determine the flow split into the two evaporators. Inside the evaporators, working fluid absorbs heat from engine exhaust and EGR, and undergoes phase changes from liquid to two-phase and then to vapor. The high-pressure and high-temperature vapor then expands through the expansion device, extracting useful work and driving either an electric generator or the engine crankshaft via gear reduction. Turbine inlet and bypass valves protect the turbine from two-phase working fluid and ensure smooth startup and shutdown of turbine expander. Finally, the working fluid vapor exiting from the expansion device flows through the condenser and transitions back to liquid phase. In the test rig, ethanol was selected as working fluid due to its favorable thermophysical properties and low global-warming potential [9]. A turbine expander with an electric generator was chosen as the expanding device due to its high thermal efficiency, wide operating range, small package volume, and low mass [10].

The ORC system is coupled to a 13L heavy duty diesel engine which is equipped with a high-pressure EGR system and a turbocharger with variable geometry turbine. The stock EGR cooler is replaced by the ORC EGR evaporator. The ORC tailpipe evaporator is placed downstream of the after-treatment system. A tailpipe evaporator bypass valve is installed in the exhaust gas path to divert a portion of the exhaust gas away from the tailpipe evaporator at high engine load conditions. The bypass valve protects the working fluid from overheat and potential degradation while also limiting heat rejection to the vehicle cooling package that would require use of the electric cooling fan. By design, the valve moves to the full bypass position at failure modes.

The 13L heavy duty diesel engine is controlled by an open ECU with an ETK interface. ECU calibration is through ETAS INCA software. The dyno control software is AVL PUMA. The ORC system is controlled by a dSPACE MicroAutoBox prototype controller. It interfaces sensors and actuators through CANSAS data acquisition system. The communication between controllers is through CAN bus.

2.2. ORC components

BorgWarner supplies the major ORC system components, including: the TP evaporator, EGR evaporator, turbine expander with electric generator, turbine expander controller, and exhaust gas bypass valve. Fig. 1b shows the pictures of above-mentioned ORC components.

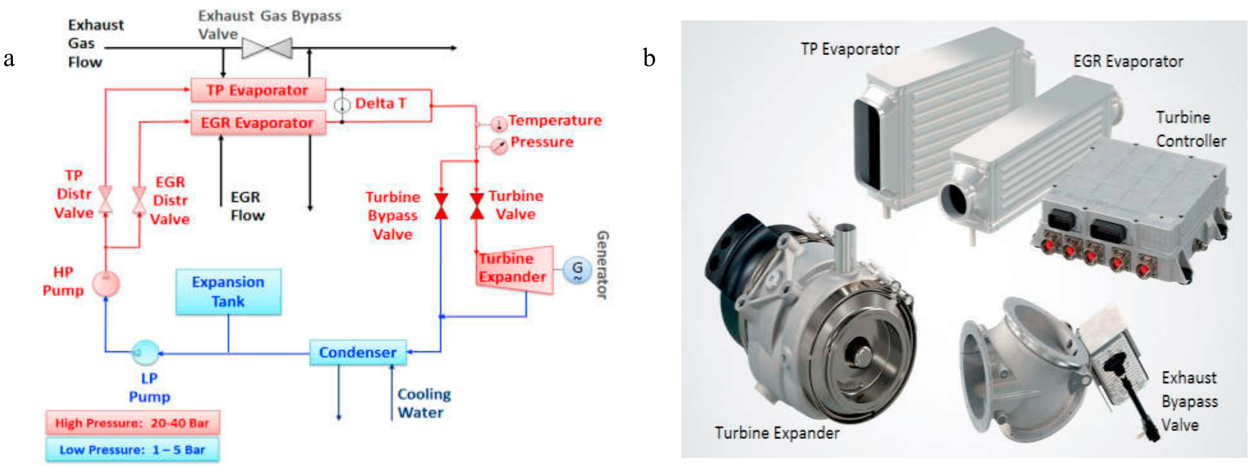

Fig. 1. (a) Schematic of ORC system with parallel evaporators [6];
(b) Main ORC system components

3. Control Development Goals and Challenges

The ORC system control development was divided into two phases. The goal of phase 1 is to achieve an operational test rig for component evaluation and system level investigation. A PID-based controller was developed to:

- achieve smooth operation during startup, steady state, and shutdown,
- ensure safe turbine operation away from 2-phase dome,
- develop safety measures including fault detection and handling of over pressure, over temperature, ethanol leak, etc.,
- transition from one operating point to another slowly.

The PID controller works well for steady state and slow transient conditions, but has difficulties in fast transients.

In phase 2, the focus is on transient cycle optimization with Model Predictive Control (MPC). The optimal setpoints of working fluid pressure and temperature are determined through offline simulations and a model predictive controller controls the pump and valves to closely track the optimal temperature and pressure setpoints.

There are many challenges in ORC system control: (i) It is a highly nonlinear Multiple Input Multiple Output (MIMO) system interfacing with the engine and dyno. (ii) Disturbances from engine exhaust flow and temperature are fast transients while the ORC working fluid temperature response to pump and valve actions is relatively slow. (iii) The time constants of EGR and TP evaporator outlet working fluid temperature response to engine speed/load change are different. The after-treatment system has large thermal inertia to smooth the exhaust gas temperature change at TP evaporator inlet, while the EGR evaporator is subject to the dynamic exhaust gas temperature change directly without a buffer. (iv) The ORC system has a wide operation range in terms of working fluid temperature and pressure. To have a controller performing well at all operating conditions, the calibration effort is significant. (v) In the two-phase region, the working fluid temperature does not vary over constant pressure, which poses difficulty in state estimation.

The ORC control is formulated as an optimal control problem with safety constraints. The following limits need to be imposed:

- Temperature limit due to dissociation and flammability of working fluid,
- Pressure limit due to structural integrity of key components,

- Vapor phase limit on turbine expander operation.

4. PID controller

The developed PID-based ORC controller enabled steady state and slow transient operation of the test rig. The working fluid pressure, temperature upstream of the turbine expander (referred to as system pressure and temperature in the sections below) and temperature differential between the two evaporator outlets (referred to as delta temperature) are key control signals. The MIMO system was divided into multiple Single Input Single Output (SISO) sub-systems. The system pressure is mainly controlled by the turbine bypass valve. The system temperature is controlled by pump speed, which correlates directly with working fluid mass flow. The delta temperature is controlled by the two mass flow distribution valves. Feed forward plus feedback PID controllers are used in system temperature and delta temperature control. The turbine speed is regulated by the generator load. Proper subcooling is achieved by adjusting the cooling water flow.

The PID controller worked well in steady-state and slow transient operations, but had difficulties in fast transient conditions due to poor disturbance rejection and undesired coupling between PID control loops. Therefore an MPC approach was adopted to improve operation during fast transients.

5. Model Predictive Control

An MPC controller was developed with a built-in evaporator model to predict future system response and generate optimal actuator commands for ORC temperature regulation and safe turbine expander operation.

5.1. Model based control development process

The model based control development follows the typical V-diagram approach. First, a high fidelity physics-based model is built and validated against experimental data. Then through model reduction techniques, the model is simplified to a reduced-order control-oriented model, which is simple enough to run in real time, yet capable to capture the main system dynamics. An optimization based controller utilizes the control-oriented model to predict future system response and generate optimal control input actions. The controller is verified with the physics-based model in offline simulations and finally validated on the test rig in real-time.

5.2. MPC controller structure

Fig. 2a shows the high-level MPC control structure. The center is the optimization based controller with a reduced-order control-oriented model. Controller objectives and constraints are predefined. The objective is to minimize temperature tracking error and control effort for a few seconds in the future. The constraints are physical limits of pump speed, temperature, pressure, valve actuation rate, etc. The optimizer calculates optimal actuator commands to minimize the objective function and then apply them to the plant model. The plant model output is feedback to the optimization-based controller. Because some system states cannot be directly measured, a state estimator is required. External disturbances, such as engine exhaust temperature and flow, are measured and fed into the controller. In the figure, x, y, u, w, r refer to state, output, input, disturbance, and reference signals respectively.

5.3. Evaporator modeling

Model predictive control requires a good plant model to predict future system response with given inputs. The key component of the ORC plant is the evaporator, where heat transfer and working fluid phase changes occur. The accuracy of the evaporator model dominates the whole ORC plant model. The major challenge is the modeling of the two-phase flow in the evaporator. Evaporator governing equations based on conservation of mass and energy within the working fluid and exhaust gas were developed in [11,6,12]. Two main evaporator modeling approaches are adopted in literature: the Finite Volume Method (FVM) and the Moving Boundary Method (MBM). In the FVM approach [13], the evaporator is discretized into many cells along the flow path. Within each cell, the working fluid properties are assumed to be homogeneous. Equations of mass and energy conservation are solved within each cell to calculate unknown flow, temperature or pressure variables. The FVM approach is not suitable for real-time control due to a large count of state variables which leads to long execution time and large memory consumption.

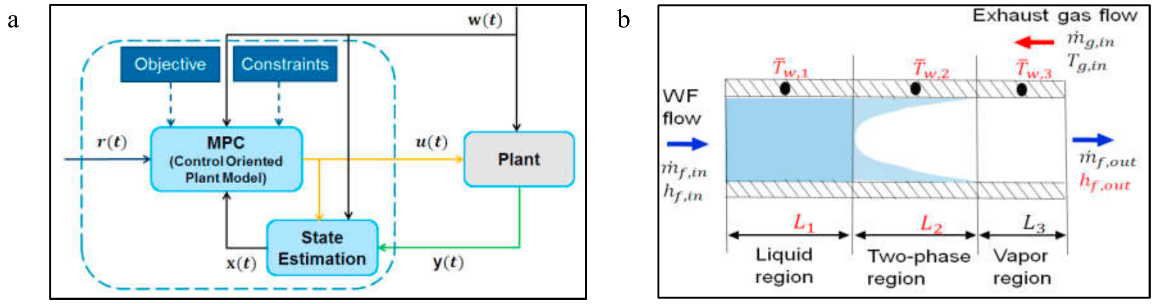

Fig. 2. (a) High-level MPC control structure; (b) Moving boundary scheme of an evaporator [6] (modified)

To reduce the computation effort in the model predictive controller, a reduced-order, control-oriented model is required. In a MBM model [11,6], the crossflow evaporator is divided by working fluid phase into liquid, two-phase and vapor regions as shown in Fig. 3b. The phase boundary locations change over time. The main concept of the MBM model is to dynamically track the boundaries of the three working fluid phases. Thermodynamic properties within each control volume are assumed to be homogenous. Within each region, conservation of mass and energy equations were derived, and system equations in state space form were developed. The state (x), input (u), disturbance (w), and output (y) vectors are listed below:

$$\begin{aligned} x &= [L_1, L_2, h_{f,out}, T_{w1}, T_{w2}, T_{w3}]' \\ u &= \dot{m}_{f,in} \\ w &= [\dot{m}_{g,in}, T_{g,in}, h_{f,in}]' \\ y &= T_{f,out} \end{aligned} \tag{1}$$

where L_1, L_2 are phase lengths of liquid region and two-phase region, $h_{f,in}, h_{f,out}$ are working fluid enthalpy at evaporator inlet and outlet, $T_{f,out}$ is working fluid temperature at evaporator outlet, T_{w1}, T_{w2}, T_{w3} are pipe surface/wall temperatures, $\dot{m}_{f,in}$ is the working fluid flow rate at evaporator inlet, and $\dot{m}_{g,in}, T_{g,in}$ are exhaust gas flow rate and exhaust gas temperature at evaporator inlet, respectively. Note that the moving boundary model considered in this paper assumes the co-existence of all three phases of working fluid along the evaporator.

Both the FVM and MBM models were correlated with test rig data and are in good agreement, more information on ORC modeling can be found in reference [12].

5.4. MPC formulation

The nonlinear system equations can be rearranged into the generic format below with state, input, and disturbance vectors defined previously. The state, input, and output variables are subject to physical constraints.

$$\begin{aligned} \dot{x}(t) &= f\big(x(t), u(t), w(t)\big) \\ y(t) &= g\big(x(t), u(t), w(t)\big) \end{aligned} \tag{2}$$

For simplification, $u_c(t)$ is defined as the combined plant input variable, comprising the $u(t)$ and $w(t)$ variables, i.e. $u_c(t) = [u(t), w(t)]^T$.

The nonlinear system equations can be linearized around a nominal operating point (x_0, u_{c0}).

$$\begin{aligned} \delta\dot{x} &= \frac{\partial f}{\partial x}\Big|_{x_0, u_{c0}} \delta x + \frac{\partial f}{\partial u_c}\Big|_{x_0, u_{c0}} \delta u_c - \dot{x}_0 = A\delta x + B\delta u_c - \dot{x}_0 \\ \delta y &= \frac{\partial g}{\partial x}\Big|_{x_0, u_{c0}} \delta x + \frac{\partial g}{\partial u_c}\Big|_{x_0, u_{c0}} \delta u_c = C\delta x + D\delta u_c \end{aligned} \tag{3}$$

where $A = \frac{\partial f}{\partial x}\big|_{x_0, u_{c0}}, B = \frac{\partial f}{\partial u_c}\big|_{x_0, u_{c0}}, C = \frac{\partial g}{\partial x}\big|_{x_0, u_{c0}}, D = \frac{\partial g}{\partial u_c}\big|_{x_0, u_{c0}}$

Since the linearized ORC system has different A, B, C, D matrix at different operating points, an adaptive linear MPC is utilized to cover the whole operating range. The adaptive MPC uses a fixed model structure, but allows the model parameters and nominal point to be updated at each control interval.

The objective or cost function is defined as

$$J = \int_{t_i}^{t_i+t_p}\left[\frac{w_t\left(T_{f,out}(\tau)-T_{sp}\right)^2}{T_{max}^2} + w_{du}\,(du(\tau))^2/du_{max}^2\right]d\tau + \frac{w_n\left(T_{f,out}(t_i+t_p)-T_{sp}\right)^2}{T_{max}^2} \quad (4)$$

Where T_{sp} is the working fluid temperature setpoint, du is the change of control input between time steps, w_t, w_{du}, w_n are weighting parameters for temperature deviation, control input change, and final temperature deviation. t_i is the current time step and t_p is the prediction time horizon. T, du are normalized in Eq. (4) so the calibration of weighting parameters is easier.

5.5. Real-time implementation of MPC on an embedded platform

The model predictive control algorithms, both adaptive Linear MPC (LMPC) and nonlinear MPC (NMPC), were implemented on a dSPACE MicroAutoBox with a 900MHz processor and 16MB RAM. LMPC was implemented using the Model Predictive Control Toolbox from Mathworks. NMPC was implemented with the ACADO Toolkit for automatic control and dynamic optimization [14]. Efficient C code of NMPC solver was generated by ACADO and integrated with the main controller in Simulink. For LMPC, unmeasurable state variables were estimated with a Kalman Filter using the exhaust gas and working fluid temperatures. For NMPC, a nonlinear estimator was constructed via an Unscented Kalman Filter (UKF) [15].

The following MPC Parameters were adopted: Measurement update time step: 0.2 sec, MPC control time step: 0.3 sec, prediction horizon steps: 50, and prediction time horizon: 15 sec. The prediction time horizon should be longer than the response time of output signal to control input step change.

Note that LMPC offers faster execution and reduced memory consumption compared with NMPC. The average computation time per step is about 10 ms for LMPC and 30 ms for NMPC. For reference, the computation time is less than 0.2ms for PID.

6. Comparison of MPC with PID

6.1. Simulation Results

The LMPC, NMPC and PID controllers were simulated with an ORC plant model with single tailpipe evaporator to evaluate the control performance. Fig. 3a shows the temperature response comparison of LMPC and PID. The y-axis is the working fluid temperature at the evaporator outlet. The engine condition is constant. The working fluid pressure is assumed constant. At 100s and 200s, the working fluid temperature setpoint has a step change of 10DegC. It can be seen that LMPC has less overshoot and shorter settling time.

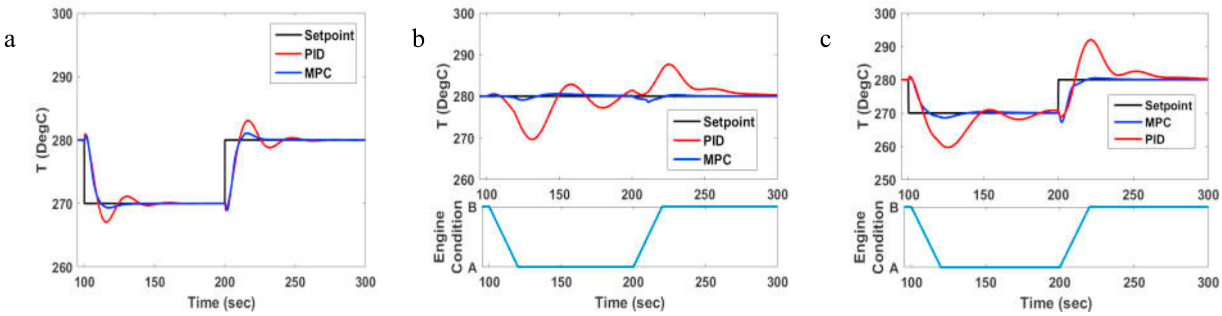

Fig. 3. Temperature responses of LMPC and PID (a) T setpoint step; (b) engine speed/load ramp; (c) T step plus engine speed/load ramp

Fig. 3b shows another simulation case, at t=100s, the engine operating condition ramps from condition B (1575RPM, 1540Nm) to condition A (1200 RPM, 1000Nm) in 20s, stays at condition A for 80s, then ramps back to condition B in 20s. The working fluid temperature set point is a constant 280C throughout the simulation. The temperature deviation from setpoint experienced with LMPC is much less than that produced with the PID controller. LMPC has better disturbance rejection.

Fig. 3c shows the evaporator outlet working fluid temperature response in a 3rd simulation case. At 100s, the engine operating condition ramps from condition B to condition A in 20 seconds. Simultaneously, the temperature set-point experiences a step change of 10DegC at 100s. LMPC regulates working fluid temperature well, while PID response exhibits a large overshoot, oscillation and longer settling time. LMPC has better temperature regulation and disturbance rejection, with fast response and minimal overshoot.

Fig. 4 shows LMPC and NMPC simulation results over a transient cycle. The bottom two curves are exhaust gas temperature and flow rate, the working fluid pump flow is controlled to achieve target temperature at evaporator outlet, 260C in this case. LMPC and NMPC produce comparable results in the simulation case. The working fluid temperature is well regulated within ± 10℃. Considering the large disturbance on the engine exhaust side in this transient cycle, the MPC performance is satisfactory.

Note that MPC has similar calibration effort to PID controller, but with significantly more modeling effort. Main tuning parameters in MPC are the weighting parameters w_t, w_{du}, w_n in Eq. (4). A larger w_{du} leads to smoother working fluid flow rate and temperature. A larger w_n leads to less steady state error. The weighting parameters are set to be constant over various engine operating conditions, and satisfactory controller performance is achieved.

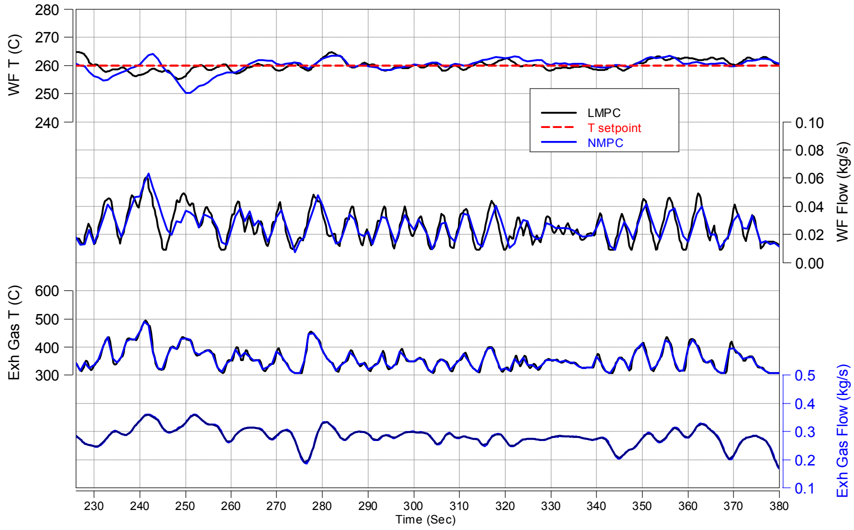

Fig. 4. Temperature regulation of LMPC and NMPC over a transient cycle

6.2. Experimental results on ORC test rig

The MPC control strategies, LMPC and NMPC, were implemented and tested on the experimental ORC rig. For the initial setup, only a single tailpipe evaporator was installed. The MPC controller regulates the working fluid temperature at the tailpipe evaporator outlet, while the PID controller controls working fluid pressure and other signals. During startup of the test rig, a predefined low pump speed was set to warmup the rig. Once the working fluid at the evaporator outlet is in vapor state, the MPC controller takes over temperature control. Fig. 5 shows the LMPC and NMPC test results of working fluid temperature response over a temperature setpoint change and an engine speed/load ramp in 60 seconds. The initial results are encouraging. The temperature step response of both LMPC and NMPC are fast and with minimal overshoot. The steady state error of working fluid temperature is small. The responses of LMPC and NMPC over transient engine operating conditions are satisfactory. The working fluid temperature is well maintained during the engine speed/load ramp test. The development is ongoing and more test results will be updated when available.

7. Conclusions and future work

An ORC test rig to recover waste heat from a heavy-duty diesel engine exhaust tailpipe and EGR system was developed. A PID based controller was developed enabling steady state and slow transient operation of the ORC system. An MPC controller was developed with a built-in evaporator model to predict future system response and generate optimal actuator commands for ORC temperature regulation. Two variants of MPC were considered, an adaptive linear MPC (LMPC) and a nonlinear MPC (NPMC). MPC showed better temperature control and improved disturbance rejection in simulation relative to PID. MPC was implemented on a real-time embedded platform. Initial test results of MPC on an ORC system with a single evaporator are encouraging. LMPC offers faster execution and reduced memory consumption compared with NMPC.

Future work includes further development and validation of the MPC controller on the ORC test rig over warmup and transient cycles. Additionally, the MPC control will be extended to an ORC system with parallel evaporators.

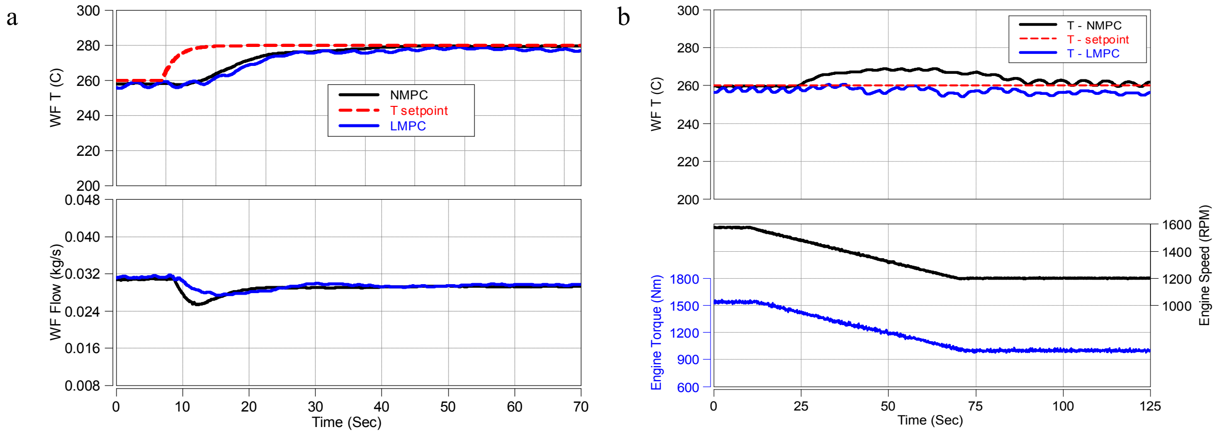

Fig. 5. (a) MPC response to T setpoint change; (b) MPC response to engine speed/load ramp on ORC test rig

References

[1] Noble A. Euro VII: The real world and its implications for OEMs and operators. IRTE Conference, 2016.
[2] Delgado O, Lutsey N. The U.S SuperTruck program: expediting the development of advanced heavy-duty vehicle efficiency technologies. The International Council on Clean Transportation, 2014.
[3] Tona P, Peralez J. Control of Organic Rankine Cycle systems on board heavy-duty vehicles: a survey. 4th IFAC Workshop on Engine and Powertrain Control, Simulation and Modeling, 2015.
[4] Endo, T, Kawajiri, S, Kojima, Y, Takahashi, K, Baba, T, Ibaraki, S, Takahashi, T, Shinohara, M. Study on maximizing exergy in automotive engines. SAE Technical Paper 2007-01-0257, 2007.
[5] Tona P, Peralez J, Sciarretta A. Supervision and control prototyping for an engine exhaust gas heat recovery system based on a steam rankine cycle. IEEE/ASME Interational Conference on Advanced Intelligent Mechatrnics, 2012.
[6] Yebi A, Xu B, Liu X, et al. Nonlinear model predictive control strategies for a parallel evaporator diesel engine waste heat recovery system. ASME. Dynamic Systems and Control Conference, 2016-9801.
[7] Feru E, Willems F, Jager B, Steinbuch M. Model predictive control of a waste heat recovery system for automotive diesel engines. 18th International Conference on System Theory, Control and Computing (ICSTCC), Sinaia, 2014, pp. 658-663.
[8] Luong D, Tsao T. Model predictive control of Organic Rankine Cycle for waste heat recovery in heavy-duty diesel powertrain. ASME Dynamic Systems and Control Conference, 2014 -5881.
[9] Seher D, Lengenfelder T, Gerhardt J, etal. Waste heat recovery for commercial vehicles with a Rankine process. 21st Aachen Colloquium Automobile and Engine Technology, 2012.
[10] Huscher F. Organic Rankine Cycle turbine expander design, development, and 48V mild hybrid system integration. 4th International Engine Congress, 2017.
[11] Jensen J. Dynamic modeling of thermo-fluid systems with focus on evaporators for refrigeration. Department of Mechanical Engineering, Technical University of Denmark, 2003.
[12] Xu B, Liu X, Shutty J, Anschel P, Onori S, Filipi Z, Hoffman M. Physics-based modeling and transient validation of an Organic Rankine Cycle waste heat recovery system for a heavy-duty diesel engine. SAE Technical Paper 0148-7191, 2016.
[13] Quoilin S, Aumann R, Grill A, Schuster A, Lemort V, Spliethoff H. Dynamic modeling and optimal control strategy of waste heat recovery Organic Rankine Cycles. Applied Energy, vol. 88, pp. 2183-2190, 2011.
[14] Houska B, Ferreau J, Diehl M. ACADO toolkit – an open source framework for automatic control and dynamic optimization. Optimal Control Applications and Methods, vol. 32, iss. 3, pp. 298-312, 2011.
[15] Yebi A, Xu B, Liu X, et al. Estimation and predictive control of a parallel evaporator diesel engine waste heat recovery system. Submitted to IEEE Transaction Control and System Technology, 2017 (under review).